Slavov, Chavdar ; Yang, Chong ; Heindl, Andreas ; Stauch, Tim ; Wegner, Hermann ; Dreuw, Andreas ; Wachtveitl, Josef

Twist and Return-Induced Ring Strain Triggers Quick Relaxation of a (Z)-Stabilized Cyclobisazobenzene

Twist and Return-Induced Ring Strain Triggers Quick Relaxation of a (Z)-Stabilized Cyclobisazobenzene
Chavdar Slavov, Chong Yang, Andreas H. Heindl, Tim Stauch, Hermann A. Wegner, Andreas Dreuw, and Josef Wachtveitl. The Journal of Physical Chemistry Letters 2018 9 (16), 4776-4781
DOI: 10.1021/acs.jpclett.8b02159

Twist and Return – Induced Ring Strain Triggers Quick Relaxation of a (*Z*)-Stabilized Cyclobisazobenzene

Chavdar Slavov,[#,1] *Chong Yang,*[#,2], *Andreas H. Heindl,*[3] *Tim Stauch,*[2,‡] *Hermann A. Wegner,*[3] *Andreas Dreuw,*[*,2] *and Josef Wachtveitl*[*,1].

[1]Institute of Physical and Theoretical Chemistry, Goethe University, Frankfurt, Germany

[2]Interdisciplinary Center for Scientific Computing (IWR), University of Heidelberg, Heidelberg, Germany

[3]Institute of Organic Chemistry, Justus Liebig University, Giessen, Germany

AUTHOR INFORMATION

Corresponding Author

* e-mail: wveitl@theochem.uni-frankfurt.de

* e-mail: dreuw@uni-heidelberg.de

[#]These authors contributed equally to this work.

[‡]Present address: Department of Chemistry, University of California, Berkeley, USA

ABSRTRACT: Continuous irradiation of the thermodynamically stable *(Z,Z)*-cyclobisazobenzene does not lead to accumulation of a *(Z,E)* or *(E,E)* isomer as one might expect. Our combined experimental and computational investigation reveals that $Z \rightarrow E$ photoisomerization still takes place on an ultrafast timescale, but induces large ring strain in the macrocycle, which leads to a very fast thermal back-isomerization preventing photo-stationary accumulation of *(E)*-isomers.

TOC GRAPHICS

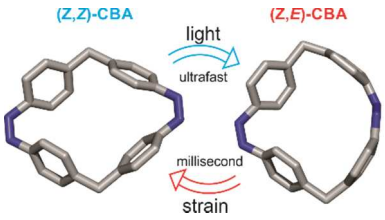

Azobenzene (AB) derivatives represent an important family of molecular photoswitches that are extensively used for spatiotemporally precise and reversible control of a variety of nanostructures[1-3] and reactions[4-5] of interest to chemistry and biology. Furthermore, ABs are used as building blocks in larger aggregates to form photoresponsive materials.[6-9] One of the main application advantages of AB photoswitches is the substantial geometrical change (molecular length change of ~3.4 Å) associated with the $E \leftrightarrow Z$ photoinduced isomerization of the central N=N bond. In addition, various AB derivatives can be prepared efficiently using a number of systematic methods.[10] ABs also show a remarkable fatigue resistance.[11]

The progress in the development of advanced photoresponsive nanostructures and materials, where multiple AB units are linked and required to operate cooperatively, demonstrates that the current understanding of the photochemistry of single ABs does not suffice to predict the behavior of more complex AB constructs. In such multi-AB constructs, the interaction between the individual photoswitching units leads to versatile effects like excitonic coupling,[12-14] extended π-delocalization,[14-16] π-stacking,[9,17] steric hindrance[18-19], and cooperativity[8,20], which all can strongly modulate the physicochemical properties of the AB units. Therefore, the rational design of photoresponsive systems requires prior, detailed investigation of all these diverse phenomena and a thorough understanding of their complexity.

Photoswitchable macrocyclic ABs[21] are a family of complex, cyclic oligo-AB constructs with great potential for application in fields like host-guest interaction,[22-23] supramolecular chemistry,[9,17,24] molecular machines,[13] and energy storage[25]. In oligo-AB macrocycles, steric distortions and ring strain alter the photoisomerization dynamics and the thermal relaxation rate of the individual AB units, and thus impact the overall photoisomerization quantum yield (QY).[22,26-27] Nevertheless, the remarkable photoswitching property of the individual ABs is

preserved in this type of compounds. However, a unique case of a minimal, strongly constraint cyclotrisazobenzene (CTA) that is locked in its (*E*,*E*,*E*)-isomer has been reported recently.[28-29] Indeed, the geometric constraints in CTA (only minimal changes of ∢CNNC are possible) transform the well-known, efficient S_1–S_0 conical intersection (CI), which typically drives the photoisomerization of ABs, into an ultrafast (<1 ps), non-photochemical relaxation pathway back to the initial isomer.[29]

To date, only a few reports exist on AB derivatives for which the (*Z*)-isomer is the thermodynamically stable form. For example in 5,6-dihydrodibenzo[c,g][1,2]diazocine,[30-31] in [0.0](3,3′)-azobenzenophane,[32] and in [1.1](4,4′)-azobenzenophane[33]. The first compound is a monomeric, bridged AB, while in the other two compounds, the (*Z*)-stable AB units are part of sterically hindered cyclic bisABs. Interestingly, $Z \rightarrow E$ photoisomerization was reported only for the former two compounds, but no (*E*)-isomer could be accumulated for [1.1](4,4′)-azobenzenophane (see chemical structure in Fig. 1), which raises the question whether [1.1](4,4′)-azobenzenophane is capable of isomerization at all or it is locked like the previously reported CTA[29]. Moreover, in the case of the two cyclic bisABs, an in-depth understanding of the molecular origin of the observed properties is still lacking. This motivated us to investigate the photoinduced dynamics of [1.1](4,4′)-azobenzenophane cyclobisazobenzene (CBA) by combining ultrafast optical spectroscopy and theoretical analysis. More fundamentally, our work contributes to the understanding of the AB photoisomerization dynamics as it reports on the ultrafast dynamics of a unique thermodynamically stable (*Z*)-AB.

The stationary absorption spectrum of the thermodynamically stable (*Z,Z*)-isomer of CBA possesses the typical (*Z*)-AB ππ*-transition (292 nm) and nπ*-transition (430 nm) bands (Fig. 1). Interestingly, the intensity of the nπ*-transition band appears to be slightly amplified in CBA as

compared to a spectral superposition of the nπ* bands of two independent monomeric (*Z*)-AB molecules. Continuous irradiation at the absorption maxima of CBA with high power LEDs or with a HgXe arc lamp did not induce any spectral changes, and thus a stationary detection of CBA $Z \rightarrow E$ photoswitching was not feasible.

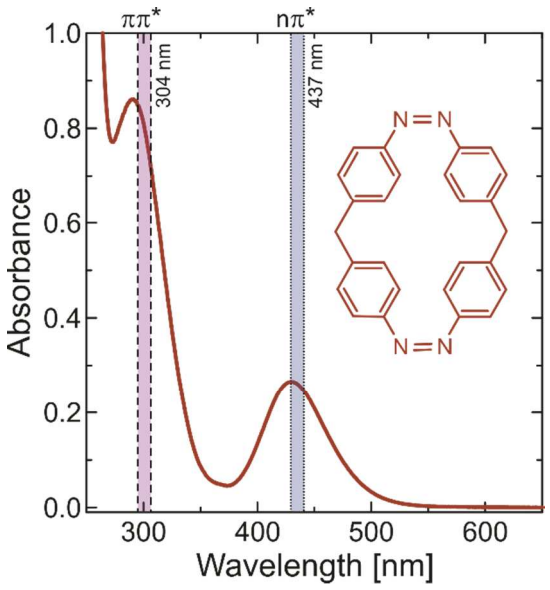

Figure 1. Experimental absorption spectrum of cyclobisazobenzene (structure shown as an inset) in ethanol. The vertical bars indicate the excitation wavelengths (304 nm and 437 nm) used in the corresponding time-resolved experiments.

Ultrafast transient absorption (TA) experiments (see Ref. [34] and the SI for a description of the experimental setup) were performed to investigate the photoinduced dynamics of *(Z,Z)*-CBA and to clarify whether the AB units of CBA have retained their isomerization capability. The TA data after excitation in the ππ*-transition band (304 nm) and after excitation in the nπ*-transition band (437 nm) show identical dynamics (Fig. 2A & 2C, see also Fig. S1), and both, indeed, reveal significant formation of the (*E*)-isomer as photoproduct. This is concluded from: *i)* the non-decaying nπ*-band ground state bleach signal (GSB) of the (*Z*)-isomer (410-450 nm, present

>1 ns); and *ii)* the absorption signals associated with the ππ* and the nπ* bands of the formed (*E*)-isomer (below 400 nm and above 450 nm). The major difference between the two datasets is found on the sub-600 fs timescale. While after ππ* excitation the sub-600 fs TA data (Fig. 2A) is dominated by excited state absorption (ESA) over the complete spectral range, after nπ* excitation the data in the 425-475 nm spectral range show a nearly instantaneous GSB of the nπ* band. Consequently, the sub-600 fs ESA contribution and its dynamics in the ππ* excitation experiment can be straightforwardly assigned to the (*Z,Z*)-CBA's ππ* excited state (conventionally labeled as S_2 in monomeric ABs). The TA data also show significant spectral overlap between the ESA bands and the (*E*)-isomer product bands, which largely conceals the early excited state relaxation, since the decaying ESA signatures transform into product absorption signatures. Nevertheless, the product absorption bands, located in the spectral ranges below 400 nm and above 450 nm, are clearly seen already <1 ps indicating ultrafast (*E*)-isomer formation after both nπ* and ππ* excitation of (*Z,Z*)-CBA.

Further insight into the early photoisomerization dynamics of (*Z,Z*)-CBA is gained via the corresponding lifetime density maps (LDM) (Fig. 2B & D), obtained from the lifetime distribution analysis of the TA data (see Ref. [35] and SI for technical details). After nπ* excitation (437 nm), the LDM (Fig. 2D) shows a series of lifetime distributions centered at ~200 fs and associated with: i) the decay of the ESA, visible at the edges of the detection spectral range; ii) the partial recovery of the GSB (400-470 nm range); and iii) the formation of the vibrationally hot (*E*)-AB product absorption bands (below 400 nm and above 450 nm). Therefore, the major decay of the nπ* excited state of *(Z,Z)*-CBA and the onset of the $Z \rightarrow E$ photoisomerization reaction occur with ~200 fs lifetime, which is similar to what was observed for monomeric (*Z*)-AB[14,30,36-37]. In previous studies on (*Z*)-AB, an additional 1-3 ps lifetime

component has been reported and assigned to diffusive motion on the nπ* PES[14,36-37] or alternatively to the decay of a dark excited state intermediate[38]. However, such a component appears to have only a minor contribution to the LDM of (*Z,Z*)-CBA (Fig. 2D), where at ~1 ps mainly the onset of the non-exponential ground state vibrational cooling dynamics[36,39] is detected as elongated and tilted lifetime distributions extending towards 10-30 ps.

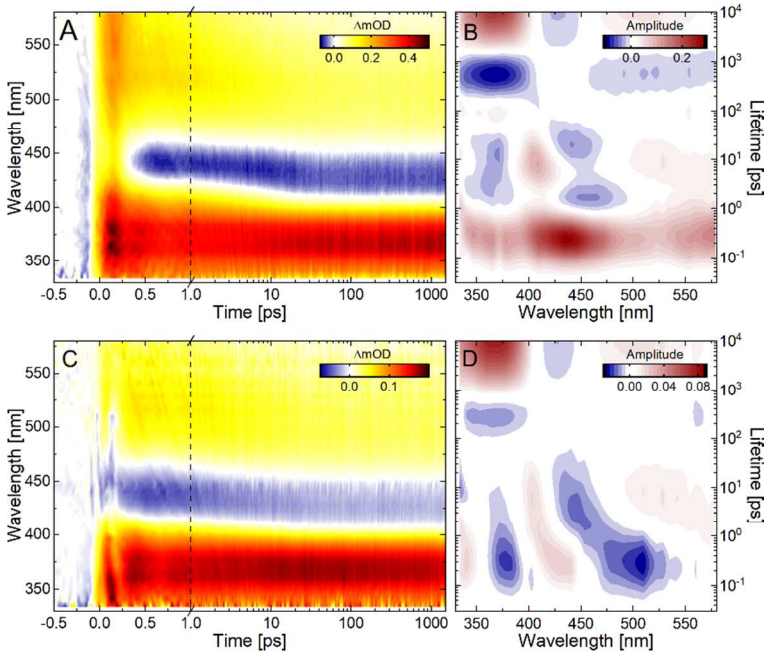

Figure 2. A) and C) Transient absorption data of the (Z,Z)-CBA measured in ethanol after 304 nm and 437 nm excitation, correspondingly (ground state bleach – negative absorption difference signal, light to dark blue; excited state and hot ground state absorption – positive absorption difference signal, yellow through red to black); B) and D) Corresponding lifetime density maps (LDMs) obtained from the lifetime distribution analysis (see SI) of the time-resolved data in A) and C). The reading of the LDMs is as for a DAS from global lifetime analysis – i) positive (red) amplitudes account for decay of absorption or rise of GSB; ii) negative (blue) amplitudes account for rise of absorption or decay of GSB.

In contrast, the LDM from the 304 nm excitation experiment (Fig. 2B) shows a pronounced positive amplitude contribution with a lifetime of ~200 fs, accounting for the decay of the ππ* excited state, comparable to what has been reported for monomeric (*Z*)-AB.[38,40] The similar decay lifetimes of the ππ* and the nπ* excited states in (*Z,Z*)-CBA does not permit their clear distinction in the ππ*-excitation experiment. Nevertheless, after the main ~200 fs decay, two minor negative lifetime distributions can be seen at ~1-2 ps, which, as described above, account for the onset of the ground state cooling commencing with the end of the relaxation of the nπ* state to the ground state. The lifetime distributions, which account well for such non-exponential behavior, reflect this situation in a more natural way. The cooling of the vibrationally hot CBA molecules in the ground state is accomplished with the characteristic 10-30 ps lifetime[36,39], as reflected by the elongated and spectrally tilted lifetime distributions on this scale (Fig. 2B & D). Additional, ~500 ps lifetime distributions (negative amplitude) are detected in the (*E)*-isomer absorption ranges (below 400 nm and above 450 nm) in both LDMs. These distributions can be linked to some conformational dynamics in the ground state that causes some modulation of the product absorption bands.

Although *(E)*-isomer of CBA could not be accumulated under stationary irradiation, the femtosecond experiments show clearly that CBA undergoes $E \rightarrow Z$ isomerization with significant quantum efficiency. Therefore, flash photolysis experiments were performed to determine the thermal $E \rightarrow Z$ relaxation of CBA, which yielded a 7.7 ms half-life for the (*E*)-isomer (Fig. S2). This high relaxation rate indicates that the formed (*E*)-configuration is significantly distorted and unstable in the electronic ground state, and therefore explains why the molecule cannot retain it.

To elucidate the molecular mechanisms of the observed photoisomerization dynamics of CBA, quantum chemical calculations were performed using time-dependent density functional theory[41-42] in combination with the BHLYP functional,[43] 6-31G* basis set,[44] and a conductor-like polarizable continuum model for ethanol solvation ($\varepsilon = 24.5$)[45] (see SI for details). Ground state geometry optimization of CBA revealed two possible geometries (see, Fig. S3 and Table S1) for each of the three isomerization states [(*Z,Z*), (*Z,E*), (*E,E*)] of CBA. These two geometries, however, are very similar and have negligible energy difference. The structural parameters (bond lengths and dihedral angles) of (*Z,Z*)-CBA closely resemble those of (*Z*)-AB (Tables S1), indicating that the thermodynamically stable isomer of CBA is only marginally, distorted compared to the isolated *(Z)*-AB. In contrast, the dihedral angles of the (*E*)-subunits in (*Z,E*)- or (*E,E*)-CBA are significantly affected and differ from undistorted *(E)*-AB. For example, the largest distortion of ∢CNNC is detected for the (*E*)-subunit in (*Z,E*)-CBA (146.6°), while in (*E,E*)-CBA both (*E*)-subunits are closer to being planar (157.3°) (Table S1). This explains why the (*Z,E*)-isomer of CBA has higher total energy than the *(E,E)*-isomer. A similar tendency is detected in the strain analysis[46-48] of CBA (see SI for details), which shows that there is hardly any strain energy (Table S2, Fig. S7) stored in the (*Z*)-subunits of both (*Z,Z*)-CBA and (*Z,E*)-CBA (the energy is similar to that of monomeric (*Z*)-AB). Conversely, tremendous molecular strain is stored in the distorted (*E*)-subunits of both (*Z,E*)-CBA and (*E,E*)-CBA – particularly in the ∢CNNC (21-30.1%), while the rest is delocalized over the benzene rings (Fig. S7). In the *(E,E)*-CBA the strain energy is shared between the two (*E*)-subunits (each stores ΔE_{harm} = ~17.7 kcal/mol, as calculated with the JEDI analysis on the basis of harmonic approximation[49-50]), however, in the (*Z,E*)-CBA this energy is almost exclusively stored in the single (*E*)-subunit, which is therefore particularly strained (ΔE_{harm} = ~27 kcal/mol) (see Table S2). The large amount

of strain in the (*E*)-subunits is the driving force of the high thermal relaxation rate (half-life 7.7 ms) observed in the flash photolysis experiments (Fig. S2) and the inability to accumulate the (*E*)-isomers under continuous irradiation.

The simulated spectra (Fig. S4) and the attachment/detachment densities (Fig. S5) show that the absorption band at 430 nm (Fig. 1) should be a superposition of the nearly degenerate nπ* transitions (S_1 and S_2) of the two (*Z*)-subunits of (*Z,Z*)-CBA. The observed slightly increased amplitude of the 430 nm absorption band (Fig. 1) indicates that the structural distortion in CBA may lead to an amplified vibronic intensity borrowing from the ππ* to the nπ* transitions. This interpretation is also supported by the optimized ground state structures of the (*Z,Z*)-isomers (Fig. S3) and the crystal structure of the molecule[33], which show that the benzene rings in CBA are slightly tilted as compared to the structure of monomeric (*Z*)-AB. In effect, the angle between the planes of the lone pair of the N-atoms and the p-orbitals of the benzene rings (see the ∢CNNC dihedral differences in Table S1) is reduced, thus possibly facilitating intensity borrowing. The higher energy transitions (S_3 and S_4) of CBA are of ππ* character (Fig. S5) and in the case of (*Z,Z*)-CBA account for the 304 nm band in the experimental absorption spectrum (Fig 1 and Fig. S4). $Z \rightarrow E$ isomerization of one AB unit leads to a red shift of the associated nπ* transition and an increased intensity (Fig. S4) due to the non-planar geometry of the (*E*)-subunit and the ensuing breaking of the C_{2h} symmetry. We observe a stronger red shift of the nπ* transition band for one of the possible (*Z,E*)-CBA ground state geometries apparently due to different interactions of the lone-pairs with the remaining nuclear frame (Fig. S3 & Fig. S4).The $Z \rightarrow E$ isomerization also induces a red shift of the ππ* transition of the (*E*)-isomer (Fig. S4) in agreement with the experimental data (Fig. 2 and Fig. S2).

To understand the unique isomerization behavior of CBA, relaxed potential energy surface (PES) scans along the rotational coordinate were performed in the S_1 ($n\pi^*$) and S_3 ($\pi\pi^*$) states of CBA (Fig. 3). The shape of the S_1 PES of both azobenzene units in CBA resembles that of the monomeric AB (cf. [51-52]). We do not observe an energetic barrier on the relaxation pathway towards the conical intersection (CI) with the ground state (Fig. 3). Furthermore, the close energetic proximity of the S_1 and the S_0 state at ∢CNNC of 80° facilitates the ultrafast excited state decay through the CI leading to isomerization via the S_1-S_0 seam already in the vicinity of this CI. On the ground state PES of the (*Z,E*)-isomer (middle of Fig. 3A), the molecular conformations towards isomerization of the remaining (*Z*)-subunit are energetically uphill. Therefore, the (*Z,E*)-isomers would predominantly reside in the local minimum on the left side of the vertical dashed line in Fig. 3A. Excitation of these populations would lead to back-isomerization since the S_1 PES shows a steeper slope towards the (*Z,Z*)-isomer, favoring the $E \rightarrow Z$ isomerization direction. If the (*Z,E*)-population in the ground state is thermally shifted towards the conformations with increasing ∢CNNC for the remaining (*Z*)-subunit, then excitation to the left side of the maximum in the S_1 PES could potentially lead to a second $Z \rightarrow E$ isomerization and formation of the (*E,E*)-isomer. However, this has not been observed so far. Concerted isomerization of the two (*Z*)-subunits of CBA is highly unlikely due to high energetic barriers on all excited states PESs in the direction of concerted $ZZ \rightarrow EE$ isomerization (see Fig. S10).

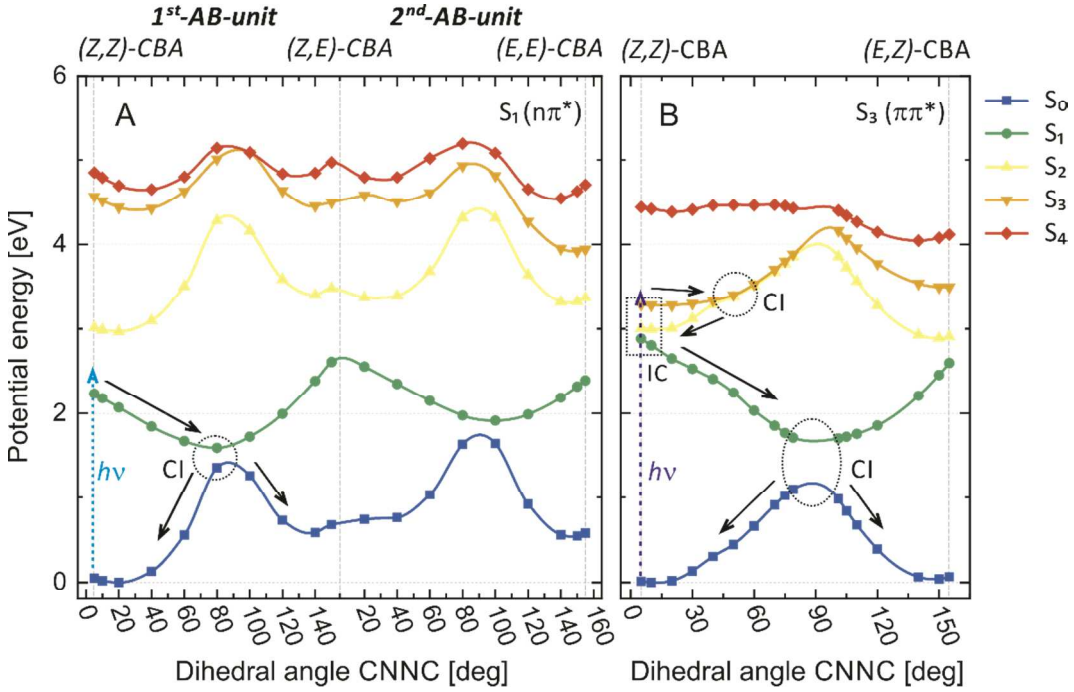

Figure 3. Potential energy surfaces for the S_1 (A) and S_3 (B) optimized geometries with constrained ∢CNNC dihedral angles at the TDDFT/BHLYP/6-31G* level of theory (For S_0 optimized PES see Fig. S8). The figures describe the photoisomerization dynamics after nπ* (A) and ππ* (B) excitation. In (A) the vertical dashed line indicates the point where the constriction of ∢CNNC is switched from the first to the second AB-unit, therefore, the possibility of consecutive isomerization from the (*Z,Z*)-isomer to the (*E,E*)-isomer after nπ* excitation is also explored. CI – conical intersection; IC – internal conversion.

The relaxed scans along the ∢CNNC rotation coordinate for the PES of the S_3 (ππ*) optimized geometry of CBA show an uphill slope toward 90° and the presence of an S_3-S_2 crossing point at ~60° of ∢CNNC (Fig. 3B). Furthermore, the S_3 and S_2 PESs lie energetically close together (see also Fig. S9). Therefore, excitation into the ππ* band (maximum at ~292 nm) would lead to a rapid S_3 relaxation to the S_2 (nπ*) PES and further to the S_1 (nπ*) PES. The subsequent S_1 state relaxation then proceeds via the pathway described above for nπ* excitation (*cf.* Fig. 3A).

In conclusion, our combined experimental and theoretical study of CBA, a model macrocyclic AB, demonstrates that the individual AB units still undergo ultrafast $Z \rightarrow E$ photoisomerization despite the strong steric hindrance in the molecule. However, the internal molecular strain, induced by the $Z \rightarrow E$ isomerization, leads to a high relaxation rate, and therefore prevents recognizable accumulation of the (*Z,E*)-isomer under continuous irradiation. Interestingly, the steric distortion in CBA, as compared to monomeric AB, breaks the molecular symmetry, which gives rise to an increased intensity of the nπ* transition due to vibronic intensity borrowing. The ultrafast dynamics, as revealed by the transient absorption experiments, indicates that the kinetics after nπ* and ππ* excitation of the (*Z,Z*)-isomer are identical after 1 ps and result in a main isomerization pathway with ~200 fs lifetime, followed predominantly by cooling dynamics in the ground state. The observed excited state dynamics is fully consistent with the computationally identified relaxation pathways for both nπ* and ππ* excitation of (*Z,Z*)-CBA. Furthermore, the computations provide a detailed insight into the molecular mechanism of the $Z \rightarrow E$ photoisomerization reaction in CBA. The results contribute to the ongoing discussion of the photoisomerization pathways of ABs. They are also particularly relevant for the design of optically active macrocycles, where tailoring of the geometric distortions and constraints within the molecule can be exploited to control the functional properties (volume, rigidity and elasticity) of macrocyclic nanostructures. From a mechanochemical perspective, the results are an important step towards triggering transformations in the environment by mechanical forces exerted by photoswitching of macrocycles.

ASSOCIATED CONTENT

Supporting Information.

The following files are available free of charge.

Supporting information containing detailed description of the experimental and theoretical methods and supporting figures. (file type, PDF)

AUTHOR INFORMATION

Corresponding author

e-mail: wveitl@theochem.uni-frankfurt.de

e-mail: dreuw@uni-heidelberg.de

Author contributions

[#]These authors contributed equally to this work.

Present address

[‡]Department of Chemistry, University of California, Berkeley, USA

ACKNOWLEDGMENT

C.S. and J.W. acknowledge funding by the DFG (WA 1850/4-2). C.Y. acknowledges the Chinese Science Council for his PhD fellowship and the support by the Heidelberg Graduate School "Mathematical and Computational Methods for the Sciences" (GSC 2020).

REFERENCES

(1) Tie, C.; Gallucci, J. C.; Parquette, J. R. Helical Conformational Dynamics and Photoisomerism of Alternating Pyridinedicarboxamide/m-(Phenylazo)azobenzene Oligomers. *J. Am. Chem. Soc.* **2006,** *128* (4), 1162.

(2) Puntoriero, F.; Ceroni, P.; Balzani, V.; Bergamini, G.; Vögtle, F. Photoswitchable Dendritic Hosts: A Dendrimer with Peripheral Azobenzene Groups. *J. Am. Chem. Soc.* **2007,** *129* (35), 10714.

(3) Steinwand, S.; Yu, Z.; Hecht, S.; Wachtveitl, J. Ultrafast Dynamics of Photoisomerization and Subsequent Unfolding of an Oligo-Azobenzene Foldamer. *J. Am. Chem. Soc.* **2016,** *138*, 12997.

(4) Donthamsetti, P. C.*, et al.* Optical Control of Dopamine Receptors Using a Photoswitchable Tethered Inverse Agonist. *J. Am. Chem. Soc.* **2017,** *139* (51), 18522.

(5) Pescher, M. D.*, et al.* Ultrafast Light-Driven Substrate Expulsion from the Active Site of a Photoswitchable Catalyst. *Angew. Chem. Int. Ed.* **2017,** *56* (40), 12092.

(6) Koskela, J. E.*, et al.* Light-Fuelled Transport of Large Dendrimers and Proteins. *J. Am. Chem. Soc.* **2014,** *136* (19), 6850.

(7) Zhou, H.*, et al.* Photoswitching of glass transition temperatures of azobenzene-containing polymers induces reversible solid-to-liquid transitions. *Nature Chemistry* **2016,** *9*, 145.

(8) Nabetani, Y.*, et al.* A Photoactivated Artificial Muscle Model Unit: Reversible, Photoinduced Sliding of Nanosheets. *J. Am. Chem. Soc.* **2011,** *133* (43), 17130.

(9) Reuter, R.; Wegner, H. A. Switchable 3D networks by light controlled π-stacking of azobenzene macrocycles. *Chem. Commun.* **2013,** *49* (2), 146.

(10) Merino, E. Synthesis of azobenzenes: the coloured pieces of molecular materials. *Chem. Soc. Rev.* **2011,** *40* (7), 3835.

(11) Bandara, H. M. D.; Burdette, S. C. Photoisomerization in different classes of azobenzene. *Chem. Soc. Rev.* **2012,** *41* (5), 1809.

(12) Röttger, D.; Rau, H. Photochemistry of azobenzenophanes with three-membered bridges. *J. Photochem. Photobiol., A* **1996,** *101* (2), 205.

(13) Norikane, Y.; Tamaoki, N. Light-Driven Molecular Hinge: A New Molecular Machine Showing a Light-Intensity-Dependent Photoresponse that Utilizes the Trans−Cis Isomerization of Azobenzene. *Org. Lett* **2004,** *6* (15), 2595.

(14) Slavov, C.*, et al.* Connectivity matters - Ultrafast isomerization dynamics of bisazobenzenes photoswitches. *Phys. Chem. Chem. Phys.* **2016,** *18*, 14795.

(15) Bahrenburg, J.*, et al.* Photochemical properties of multi-azobenzene compounds. *Photochem. Photobiol. Sci.* **2013,** *12* (3), 511.

(16) Floß, G.; Saalfrank, P. The Photoinduced E → Z Isomerization of Bisazobenzenes: A Surface Hopping Molecular Dynamics Study. *J. Phys. Chem. A* **2015,** *119* (20), 5026.

(17) Norikane, Y.; Hirai, Y.; Yoshida, M. Photoinduced isothermal phase transitions of liquid-crystalline macrocyclic azobenzenes. *Chem. Commun.* **2011,** *47* (6), 1770.

(18) Titov, E.; Granucci, G.; Götze, J. P.; Persico, M.; Saalfrank, P. Dynamics of Azobenzene Dimer Photoisomerization: Electronic and Steric Effects. *J. Phys. Chem. Lett.* **2016,** *7* (18), 3591.

(19) Valley, D. T.; Onstott, M.; Malyk, S.; Benderskii, A. V. Steric Hindrance of Photoswitching in Self-Assembled Monolayers of Azobenzene and Alkane Thiols. *Langmuir* **2013,** *29* (37), 11623.

(20) Weber, C.*, et al.* Cooperative Switching in Nanofibers of Azobenzene Oligomers. *Sci. Rep.* **2016,** *6*, 25605.

(21) Wagner-Wysiecka, E.; Łukasik, N.; Biernat, J. F.; Luboch, E. Azo group(s) in selected macrocyclic compounds. *Journal of Inclusion Phenomena and Macrocyclic Chemistry* **2018**.

(22) Norikane, Y.; Kitamoto, K.; Tamaoki, N. Novel Crystal Structure, Cis−Trans Isomerization, and Host Property of Meta-Substituted Macrocyclic Azobenzenes with the Shortest Linkers. *J. Org. Chem.* **2003,** *68* (22), 8291.

(23) Ryan, S. T. J.; Barrio, J. d.; Suardíaz, R.; Ryan, D. F.; Rosta, E.; Scherman, O. A. A Dynamic and Responsive Host in Action: Light Controlled Molecular Encapsulation. *Angew. Chem. Int. Ed.* **2016,** *55* (52), 16096.

(24) Shen, Y.-T.; Guan, L.; Zhu, X.-Y.; Zeng, Q.-D.; Wang, C. Submolecular Observation of Photosensitive Macrocycles and Their Isomerization Effects on Host−Guest Network. *J. Am. Chem. Soc.* **2009,** *131* (17), 6174.

(25) Durgun, E.; Grossman, J. C. Photoswitchable Molecular Rings for Solar-Thermal Energy Storage. *J. Phys. Chem. Lett.* **2013,** *4* (6), 854.

(26) Bassotti, E.*, et al.* Effect of Strain on the Photoisomerization and Stability of a Congested Azobenzenophane: A Combined Experimental and Computational Study. *J. Phys. Chem. A* **2006,** *110* (45), 12385.

(27) Schweighauser, L.; Häussinger, D.; Neuburger, M.; Wegner, H. A. Symmetry as a new element to control molecular switches. *Org. Biomol. Chem.* **2014,** *12* (21), 3371.

(28) Reuter, R.; Hostettler, N.; Neuburger, M.; Wegner, H. A. Synthesis and Property Studies of Cyclotrisazobenzenes. *Eur. J. Org. Chem.* **2009,** (32), 5647.

(29) Slavov, C.; Yang, C.; Schweighauser, L.; Wegner, H. A.; Dreuw, A.; Wachtveitl, J. Ultrafast Excited-State Deactivation Dynamics of Cyclotrisazobenzene—A Novel Type of UV-B Absorber. *ChemPhysChem* **2017,** *18* (16), 2137.

(30) Siewertsen, R.*, et al.* Highly Efficient Reversible Z-E Photoisomerization of a Bridged Azobenzene with Visible Light through Resolved S-1(n pi*) Absorption Bands. *J. Am. Chem. Soc.* **2009,** *131* (43), 15594.

(31) Siewertsen, R.; Schonborn, J. B.; Hartke, B.; Renth, F.; Temps, F. Superior Z → E and E → Z photoswitching dynamics of dihydrodibenzodiazocine, a bridged azobenzene, by S1(nπ*) excitation at λ = 387 and 490 nm. *Phys. Chem. Chem. Phys.* **2011,** *13* (3), 1054.

(32) Norikane, Y.; Katoh, R.; Tamaoki, N. Unconventional thermodynamically stable cis isomer and trans to cis thermal isomerization in reversibly photoresponsive [0.0](3,3[prime or minute])-azobenzenophane. *Chem. Commun.* **2008,** (16), 1898.

(33) Heindl, A. H.; Schweighauser, L.; Logemann, C.; Wegner, H. A. Azobenzene Macrocycles: Synthesis of a Z-Stable Azobenzenophane. *Synthesis* **2017,** *49* (12), 2632.

(34) Slavov, C., *et al.* Ultrafast coherent oscillations reveal a reactive mode in the ring-opening reaction of fulgides. *Phys. Chem. Chem. Phys.* **2015,** *17*, 14045.

(35) Slavov, C.; Hartmann, H.; Wachtveitl, J. Implementation and evaluation of data analysis strategies for time-resolved optical spectroscopy. *Anal. Chem.* **2015,** *87* (4), 2328.

(36) Nägele, T.; Hoche, R.; Zinth, W.; Wachtveitl, J. Femtosecond photoisomerization of cis-azobenzene. *Chem. Phys. Lett.* **1997,** *272* (5-6), 489.

(37) Satzger, H.; Spörlein, S.; Root, C.; Wachtveitl, J.; Zinth, W.; Gilch, P. Fluorescence spectra of trans- and cis-azobenzene - emission from the Franck-Condon state. *Chem. Phys. Lett.* **2003,** *372* (1-2), 216.

(38) Quick, M., *et al.* Photoisomerization Dynamics and Pathways of trans- and cis-Azobenzene in Solution from Broadband Femtosecond Spectroscopies and Calculations. *J. Phys. Chem. B* **2014,** *118* (29), 8756.

(39) Hamm, P.; Ohline, S. M.; Zinth, W. Vibrational cooling after ultrafast photoisomerization of azobenzene measured by femtosecond infrared spectroscopy. *J. Chem. Phys.* **1997,** *106* (2), 519.

(40) Satzger, H.; Root, C.; Braun, M. Excited-State Dynamics of trans- and cis-Azobenzene after UV Excitation in the ππ* Band. *J. Phys. Chem. A* **2004,** *108* (30), 6265.

(41) Casida, M. E. *Recent Advances in Density Functional Methods*. World Scientific: 1995; Vol. Part I.

(42) Dreuw, A.; Head-Gordon, M. Single-Reference ab Initio Methods for the Calculation of Excited States of Large Molecules. *Chem. Rev.* **2005,** *105* (11), 4009.

(43) Becke, A. D. A new mixing of Hartree–Fock and local density functional theories. *J. Chem. Phys.* **1993,** *98* (2), 1372.

(44) Hehre, W. J.; Ditchfield, R.; Pople, J. A. Self—Consistent Molecular Orbital Methods. XII. Further Extensions of Gaussian—Type Basis Sets for Use in Molecular Orbital Studies of Organic Molecules. *J. Chem. Phys.* **1972,** *56* (5), 2257.

(45) Liu, J.; Liang, W. Analytical second derivatives of excited-state energy within the time-dependent density functional theory coupled with a conductor-like polarizable continuum model. *J. Chem. Phys.* **2013,** *138* (2), 024101.

(46) Daoust, K. J.; Hernandez, S. M.; Konrad, K. M.; Mackie, I. D.; Winstanley, J.; Johnson, R. P. Strain Estimates for Small-Ring Cyclic Allenes and Butatrienes. *The Journal of Organic Chemistry* **2006,** *71* (15), 5708.

(47) Wheeler, S. E.; Houk, K. N.; Schleyer, P. v. R.; Allen, W. D. A Hierarchy of Homodesmotic Reactions for Thermochemistry. *J. Am. Chem. Soc.* **2009,** *131* (7), 2547.

(48) Stauch, T.; Dreuw, A. Quantum Chemical Strain Analysis For Mechanochemical Processes. *Acc. Chem. Res.* **2017,** *50* (4), 1041.

(49) Stauch, T.; Dreuw, A. A quantitative quantum-chemical analysis tool for the distribution of mechanical force in molecules. *J. Chem. Phys.* **2014,** *140* (13), 134107.

(50) Stauch, T.; Dreuw, A. On the use of different coordinate systems in mechanochemical force analyses. *J. Chem. Phys.* **2015,** *143* (7), 074118.

(51) Weingart, O.; Lan, Z.; Koslowski, A.; Thiel, W. Chiral Pathways and Periodic Decay in cis-Azobenzene Photodynamics. *J. Phys. Chem. Lett.* **2011,** *2* (13), 1506.

(52) Tiago, M. L.; Ismail-Beigi, S.; Louie, S. G. Photoisomerization of azobenzene from first-principles constrained density-functional calculations. *J. Chem. Phys.* **2005,** *122* (9), 094311.